Available online at www.sciencedirect.com
SCIENCE DIRECT®
International Journal of Heat and Mass Transfer 48 (2005) 5395–5407
International Journal of HEAT and MASS TRANSFER
www.elsevier.com/locate/ijhmt

Delay of wetting propagation during jet impingement quenching for a high temperature surface

Aloke Kumar Mozumder [a,1], Masanori Monde [a,*], Peter Lloyd Woodfield [b,2]

[a] Department of Mechanical Engineering, Saga University, 1 Honjo-machi, Saga 840-8502, Japan
[b] Institute of Ocean Energy, Saga University, 1 Honjo-machi, Saga 840-8502, Japan

Received 5 October 2004
Available online 26 September 2005

Abstract

Transient heat transfer has been investigated experimentally with a subcooled water jet during quenching of hot cylindrical blocks made of copper, brass and steel for initial surface temperatures from 250 to 400 °C. The jet velocity was from 3 to 15 m/s and jet subcooling from 5 to 80 K with a jet diameter of 2 mm. When the jet strikes the hot surface, the wetting front becomes stagnant for a certain period of time in a small central region before wetting the entire surface. This wetting delay may be described as the resident time which is a strong function of block material and jet subcooling and also a function of initial block temperature and jet velocity. New correlations for the resident time and the surface temperature at the resident time at the wetting front have been proposed.

Keywords: Quenching; Resident time; Inverse solution; Impinging jet

1. Introduction

Jet impingement quenching is widely employed having many industrial applications relating to rapid cooling and better control of high temperatures. In the manufacturing world, jet cooling is used in processes such as extrusion, casting, forging and annealing for the purpose of having precise mechanical and metallurgical properties. Spray nozzle and impinging cooling are coming into wider use for removing of heat from electronic chips also. In water-cooled nuclear reactors, it is essential to control the heat removal rate from the fuel element during a loss of coolant accident (LOCA). At that time the fuel element will overheat even though the reactor is immediately shutdown. In the event of such an emergency it is necessary to provide an alternative cooling system known as emergency core cooling (ECC). For the purpose of emergency core cooling, water jets are impinged on the hot fuel element. In certain types of water-cooled reactors, this emergency cooling water is sprayed into each fuel bundle from a pipe situated in the centre of the bundle. When a jet of emergency cooling water impinges on a hot fuel element, stable film boiling occurs [1]. Convective and radiative heat transfer locally remove the stored heat and after a time (the wetting delay time or resident time) the film

* Corresponding author. Tel.: +81 952 28 8608; fax: +81 952 28 8587.
E-mail addresses: 03ts11@edu.cc.saga-u.ac.jp (A.K. Mozumder), monde@me.saga-u.ac.jp (M. Monde), peter@me.saga-u.ac.jp (P.L. Woodfield).
[1] Tel.: +81 952 28 3216; fax: +81 952 28 8595.
[2] Tel.: +81 952 26 3870; fax: +81 952 28 8595.

0017-9310/$ - see front matter © 2005 Elsevier Ltd. All rights reserved.
doi:10.1016/j.ijheatmasstransfer.2005.06.034

Nomenclature

a	thermal diffusivity (m^2/s)
c	specific heat (kJ/kg K)
d	jet diameter (mm)
$f(\tau,\gamma,\zeta_n)$	function for depicting temperature variation on plane $\zeta=\zeta_n$ beneath the surface
$G_{j,k}^{(m,n)}$	coefficient in Eq. (2)
$H_{j,k}^{(m,n)}$	coefficient in Eq. (3)
$J_0(r)$, $J_1(r)$	Bessel function
l_r	length in r direction of a cylindrical coordinate (mm)
l_z	length in z direction of a cylindrical coordinate (mm)
m_j	eigenvalue (root of $J_1(m_j)=0$)
m	mass flow rate of liquid
N	order of approximating polynomial
N_j	number of eigenvalues minus one
$P_{j,k}^{(n)}$	coefficient derived from measured temperature variation
q_w	surface heat flux (MW/m^2)
r	position in the radial direction of the block (mm)
r^*	radial position of wetting front at resident time (mm)
T	measured temperature (mm)
t	time (counted from the impingment of jet) (s)
t^*	resident time (s)
T^*	solid–liquid interface temperature (°C)
T_b	block initial temperature (°C)
T_{liq}	liquid temperature (°C)
T_{sat}	saturated temperature (°C)
T_w	surface temperature (°C)
T_w^*	surface temperature at resident time (at $r=r^*$) (°C)
u	jet velocity (m/s)
z	z-coordinate distance (in axial direction of the cylinder) (mm)
z_1, z_2	the distance of thermocouples location from the hot surface (mm)

Greek symbols

ΔT	thermal potential (K)
ΔT_{sub}	liquid subcooling ($=T_{sat}-T_{liq}$)
θ_w	non-dimensional surface temperature (T/T_b)
Φ_w	non-dimensional surface heat flux
λ	thermal conductivity (kW/m K)
τ	non-dimensional time (at/l_r^2)
ζ	non-dimensional distance in z direction (z/l_z)
γ	non-dimensional distance in r direction (r/l_r)
ρ	density (kg/m^3)
τ_n^*	non-dimensional time lag

Subscripts

l	liquid
s	solid

becomes unstable and a wet patch is initiated. This wet patch spreads and results in the formation of a stable quenching front. Understanding of the wetting delay or resident time, which occurs between jet initiation and starting of wetting front movement, is of great importance in analyzing the consequences of a loss of coolant accident. This delay time influences the total time to quench the fuel bundle and, if long can lead to excessive cladding temperatures or in the worst case a failure of the emergency cooling system. In order to investigate this wetting delay phenomena an experimental study on jet impingement quenching for a high temperature surface has been conducted.

Due to increasing demand for utility of quenching in industry, researchers and scientists have carried out analytical and experimental investigations for clear understanding of quenching phenomena. Quenching can be defined as a heat transfer process in which extremely rapid cooling results from bringing a high temperature solid into sudden contact with a lower temperature fluid. Generally, the key feature responsible for the rapid cooling is a rewetting process which is believed to occur when the temperature of the hot surface is below a certain value referred as the rewetting, sputtering or Leidenfrost temperature. However, the Leidenfrost temperature does not appear to be a simple function of the liquid properties. Moreover, the mechanism for defining this temperature, if a single mechanism actually exits, is not well established and numerous proposals have been made [2]. Studies of jet impingement quenching for multiphase heat transfer have been performed by many researchers [2–7]. Heat flux, temperature, and the flow field by flow visualization were studied extensively in those investigations. Some other studies [8–10] also performed on free surface jet impingement cooling, have given valuable background information on single phase convection heat transfer. Wetting delay is an important phenomena in jet impingement quenching. Only a few publications however are available still now. In this article, the initiative has been taken to investigate this relatively unexplored field.

Piggott et al. [11] experimentally investigated wetting delay during cooling of a hot rod using a subcooled water jet. During the quench, constant power was sup-

plied to the rods corresponding to that initially necessary to maintain a steady temperature in air before the jet was applied. In the present study, the jet was impinged for cooling of a flat surface and no power was supplied during quenching. Owen and Pulling [1] presented a model for the transient film boiling of water jets impinging on a hot metal surface of stainless steel and nimonic alloy. In their study, wetting of the surface was assumed to occur when the temperature of the surface falls to the Leidenfrost temperature. Kumagai et al. [12] conducted an experimental investigation of cooling a hot thick copper plate by impinging a plane water jet to clarify the transient behaviour of boiling heat transfer performance along the surface and the temperature profile inside the body as well as on the surface. This experimental result indicated a time delay of approximately 100 s before the movement of the wetting front for a saturated jet with velocity 3.5 m/s and an initial solid temperature of 400 °C. Hammad [13] reported resident times for subcooled jet impinging on block with different initial solid temperatures, 250 °C and 300 °C. While these studies have shed some qualitative light on the subject, there is an urgent need to clarify under what circumstances the wetting front will move forward and to develop practical correlations to estimate the resident time as a function of initial solid temperature, jet velocity, temperature of liquid, solid and liquid properties and solid geometry. This goal is by no means an easy task due to the complex nature of the problem.

After the jet impingement and before the wetting front movement many complicated processes and subprocesses have been observed [14,15]. During this time, dramatic changes in the flow pattern depending on the superheat of the surface and possibly homogeneous nucleate boiling in the case of higher interface temperatures have been reported [14]. In this study, when the block temperature was higher than 300 °C, an almost explosive flow pattern was reported and a conical sheet of liquid in the case of slightly lower temperatures was observed. For the gradual cooling of a high temperature surface, both patterns were observed within the resident time, initially explosive and then the liquid sheet. In this case, the intensity level of the boiling sound was found to decrease and the rate of heat transfer increased when the flow field changed from the explosive pattern to the sheet pattern [15]. The main objectives of Ref. [15] were mainly to represent the flow patterns before and after the resident time. The present study deals with the resident time itself, its dominating parameters and their relation.

Just at the moment when the wetting front starts moving, the surface temperature and the other dominating parameters are favorable for the wetting front to move quickly towards the circumference of the hot surface. However, exactly which parameters define a favorable wetting condition is presently uncertain. In contrast to the resident time, once the wetting front starts moving it does not take much time to completely cover the surface [6]. Hammad et al. [6] found that for any experimental condition they considered, the heat flux reaches its maximum value just after the wetting front starts moving rather than when the jet first strikes the block. Therefore in parallel with the resident time, the time required to reach the maximum heat flux condition is a strong function of the liquid subcooling and jet velocity. Thus the resident time is very important because this time also gives an indication of the time required to reach the maximum heat flux situation.

The objectives of the present study are to investigate the parameters which control the resident time and the surface temperature at the wetting front at that time. An attempt has been made to correlate the parameters considered with resident time and temperature. In particular, three different solid materials, four jet velocities, four subcoolings and four initial solid temperatures have been included.

2. Experimental apparatus and procedure

The experimental set-up shown in Fig. 1 contains five major components, a heated block, a fluid flow system, a data acquisition system, a high-speed video camera and a sound measuring unit. At the beginning of the experiment, the water container (3) is filled with distilled water up to a certain level which can be seen through the level gauge (20). The pump (6) produces a water jet through the nozzle (10) of diameter 2 mm, which is located centrally 44 mm from the test surface (1). A shutter (24) is mounted in front of the nozzle to prevent water from striking the block (1) prematurely and to maintain a constant water temperature by forcing it to run within a closed loop system. The desired temperature of the water is obtained by controlling the main heater (4), auxiliary heater (7) or by adding cooling water (23) to the heat exchanger (5). The desired initial temperature of the block (1) is achieved by heating it with an electrical heater mounted around the block. A dynamic strain meter (12) is attached at two points of the flow line before the nozzle for measuring differential pressure (11) from which jet velocity is calculated and this velocity is adjusted by a regulating valve (8). Nitrogen gas is fed around the heated surface by opening the cylinder valve (19) to create an inert atmosphere and consequently, prevent oxidization of the test surface. The whole experiment is conducted at one atmosphere pressure. When all the desired experimental conditions are fulfilled, then the shutter (24) is opened for the water jet to strike the center of the flat surface of the heated block. The high speed video camera (17) starts simultaneously at the signal of opening shutter to record the flow pattern over the heated block surface and at the

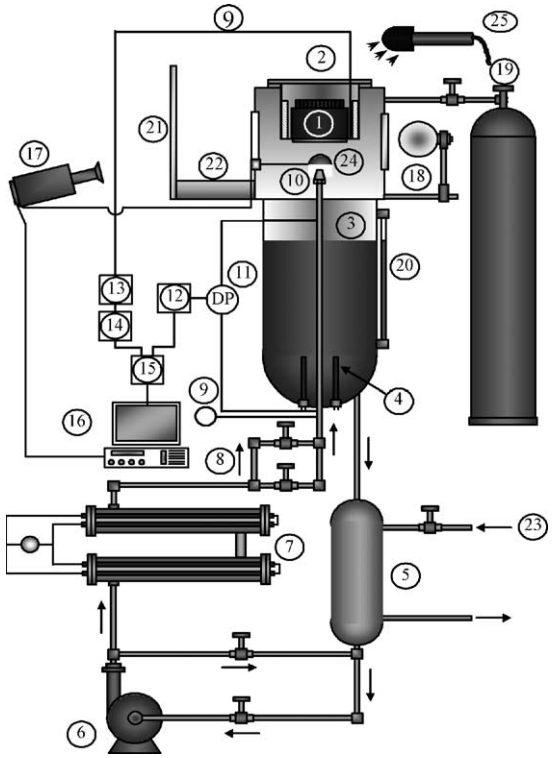

Fig. 1. Schematic diagram of the experimental set-up. (1) Tested block, (2) block holder, (3) liquid tank, (4) heater, (5) heat exchanger, (6) pump, (7) auxiliary heater, (8) regulating valve, (9) thermocouple, (10) nozzle, (11) differential pressure, (12) dynamic strain meter (for measuring jet velocity), (13) ice box, (14) voltage amplifier, (15) A/D converter, (16) computer, (17) high-speed video camera, (18) spot light, (19) nitogen cylinder, (20) level gauge, (21) glass frame, (22) vessel, (23) cooling water, (24) rotary shutter, (25) microphone.

same time, the 16 thermocouples measure the temperatures inside the heated block. Sound has been also recorded simultaneously at the same time with the microphone (25) for some conditions.

Table 1 shows the experimental conditions of the present study. For different experiments, ±2 °C deviation from the desired initial block temperature was allowed. The jet velocity could be set to an accuracy of ±0.1 m/s. The initial temperature of the liquid before the run of the experiment could be controlled to within 1 °C from the set point. However, for long cooling conditions, during the experimental run, it was difficult to maintain the initial liquid temperature. Sometimes, ±2 °C variation from the initial temperature occurred.

2.1. Heated block

The heated block is of cylindrical shape with 94 mm diameter and 59 mm height as shown in Fig. 2. In order to make it easy to fix the thermocouples inside the heated block, a small section of the block was made removable but no cuts were made through the test surface itself. The effect of this removable section is limited to one corner of the block in an area more than $r = 30$ mm, where it is found from video observation that there is a departure from symmetry in the expanding of the wetting front. Therefore, all data reported in this study are for radial positions less than $r = 30$ mm where the results may be considered axisymmetric. Sixteen thermocouples (CA-type, 1 mm sheath diameter and 0.1 mm wire diameter) are located at two different depths, 2.1 mm and 5 mm from the surface as described elsewhere [16]. At each depth, eight thermocouples are inserted along the r-axis. To protect the heated test surface from oxidation, it was plated with a thin layer of gold, 16 μm, which has an excellent oxidation resistance and also a good thermal conductivity; $\lambda \approx 317$ W/m K. The surface roughness is 0.2–0.4 μm. Fig. 2 shows the assembly of the block, where it is mounted in a block holder and is heated by an electrical sheath heater with

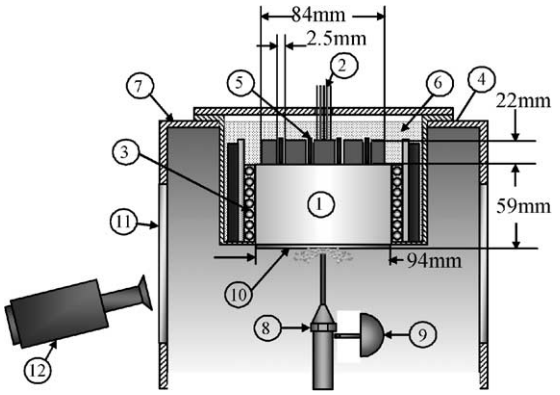

Fig. 2. Schematic diagram of the test section and heating element. (1) Tested block, (2) thermocouples, (3) sheath heater, (4) band type heater, (5) slot type heater, (6) glass wool, (7) block holder, (8) nozzle, (9) rotary shutter, (10) 16 μm gold plated test surface, (11) glass window, (12) high speed video camera.

Table 1
Experimental conditions of the present study

Block material	Initial temperature, T_b [°C]	Jet velocity, u [m/s]	Jet sub-cooling, ΔT_{sub} [K]
Copper, brass, steel	400, 350, 300, 250	15, 10, 5, 3	80, 50, 20, 5

0.94 kW capacity, that is coiled around the block circumference. To thermally insulate the block and to keep a uniform heat flux at the surfaces, two auxiliary heaters are used; one of them is of band type, 0.65 kW, and is placed around the block circumference, while the second is of slot type, 0.5 kW, and is placed in the four groves in the upper part of the block as illustrated in Fig. 2.

2.2. Data acquisition system

The thermocouples are scanned sequentially at 0.05 s intervals, with 8.0 ms needed to read all of the thermocouples using 16-bit resolution with an analog–digital converter. The duration of the total data acquisition period was adjusted to suit the experimental conditions so that in all cases the experiment continued until the quench was completed. The uncertainty in the temperature measurements is ±0.1 °C, while the uncertainty in the placement of the thermocouples is estimated to be ±0.1 mm. The time lag for the response of the thermocouples is estimated to be less than 0.1 s.

2.3. Analysis of the experimental data

The inserted thermocouples measured the temperatures beneath the hot surface onto which the jet impinged. This procedure was necessary since during the quenching it was impossible to measure the temperature at the surface directly. An analytical solution to the inverse heat conduction problem was then applied to estimate the surface temperature and surface heat flux based on the measured temperatures beneath the test surface. The two-dimensional inverse solution for heat conduction used in this report was adopted from Monde et al. [17] and Hammad et al. [18]. At two depths 2.1 mm and 5 mm from the surface, a total of 16 thermocouples (eight thermocouples at each depth) were inserted which recorded temperatures during quenching. For the best spatial resolution, 28–30 eigenvalues have been recommended [16] which required that additional points be added in the radial direction. Extra points were interpolated by using a smooth spline method to increase the number of reference points to 29. After following the same procedure for both the depths, the following approximate equation, Eq. (1), was applied for each distance:

$$f(\tau,\gamma,\zeta_n)=\sum_{j=0}^{N_j}J_0(m_j\gamma)\cdot\sum_{k=0}^{N}\frac{P_{j,k}^{(n)}\cdot(\tau-\tau_n^*)^{k/2}}{\Gamma(k/2+1)}\quad \text{at } n=1,2 \tag{1}$$

The least squares method was then applied with the help of the measured temperatures to determine the coefficients $P_{j,k}^{(n)}$. After verification of the applicability of coefficients in Eq. (1) by comparison with the original measured distributions, they were then used to explicitly calculate the surface temperature (Eq. (2)) and heat flux (Eq. (3)):

$$\theta_w(\tau,\gamma)=\sum_{j=0}^{N_j}\sum_{\ell=-1}^{N}G_{j,\ell}^{(1,2)}\cdot\frac{(\tau-\tau_1^*)^{\ell/2}}{\Gamma(\ell/2+1)}\cdot J_0(m_j\gamma)-\sum_{j=0}^{N_j}\sum_{\ell=-1}^{N}G_{j,\ell}^{(2,1)}\cdot\frac{(\tau-\tau_2^*)^{\ell/2}}{\Gamma(\ell/2+1)}\cdot J_0(m_j\gamma) \tag{2}$$

$$\Phi_w(\tau,\gamma)=\sum_{j=0}^{N_j}\sum_{\ell=-1}^{N}H_{j,\ell}^{(1,2)}\cdot\frac{(\tau-\tau_1^*)^{\ell/2}}{\Gamma(\ell/2+1)}\cdot J_0(m_j\gamma)-\sum_{j=0}^{N_j}\sum_{\ell=-1}^{N}H_{j,\ell}^{(2,1)}\cdot\frac{(\tau-\tau_2^*)^{\ell/2}}{\Gamma(\ell/2+1)}\cdot J_0(m_j\gamma) \tag{3}$$

where $\mathrm{erfc}(\gamma_n/2\sqrt{\tau_n^*})=\min(\theta)$ and here, $\min(\theta)$ is the minimum readable division of measured temperature. The mathematical derivation of this inverse solution and the method to determine the coefficients in Eqs. (2) and (3) have been discussed in detail by Monde et al. [17] and Hammad et al. [18]. The values of $N=5$ and $N_j=28$ were used here which were enough for an accurate result as was numerically verified by Hammad et al. [18].

In this study, the resident time has been estimated on the basis of two independent ways, one is when the surface temperature starts dropping quickly and the other is from the video images when the wetting front starts moving. In most of the cases both agree well. Since video recording was not made for every case, only the first means was sometimes employed to estimate the resident time. The accuracy for the smaller value of resident time (and the corresponding surface temperature when the wetting front starts moving) is low especially for the resident time less than 1 s. This is because it is difficult to detect exactly when the wetting front starts moving.

2.4. Visual observation

Fluid movement over the heated surface during the quenching was captured by a high-speed video camera. Pictures with a maximum resolution of 1280 × 1024 pixels and a maximum rate of 10,000 frames/s. From individual frames of the video images, the wetting front movement and the splattering of liquid droplets were analyzed.

2.5. Audible observation

For some cases, a microphone was simultaneously employed during quenching to record the sound. The recorded sound signal (electrical voltage) was then normalized against the peak voltage during the recording giving a representation of noise level before and after the wetting front propagation.

3. Results and discussion

3.1. Definition of resident time

Before proceeding with the discussion it is important to clarify the meaning of the key parameter for the present investigation. The resident time, t^*, in the present study is defined as the time from when the jet first strikes the hot surface until the wetting front starts moving. It can be thought of as the time during which the wetting front or region of interaction between the jet and hot solid is residing at or near the center. The expression 'resident time' in connection with jet quenching first appeared in the work of Hammad [13] and is synonymous to 'wetting delay time' used by Piggot et al. [11]. The resident time should not be thought of as purely a film boiling time since the present observations clearly indicate that surface wetting in the central region can occur a considerable time before movement of the wetting front.

3.2. Visual and audible observations before and after wetting front movement

For conditions where the material was copper or brass, the initial temperature was high, the jet velocity was low and the subcooling was low, when the jet first struck the center of the hot surface, liquid did not cover the entire heated area immediately. Rather as is shown in Fig. 3(a) the liquid quickly spread over a small central region about two to four times the jet diameter and then was splashed out or deflected away from the surface. The size of this region of liquid/solid interaction remained relatively fixed for a considerable period of time. Finally the wetting front began to move across the surface as in Fig. 3(b).

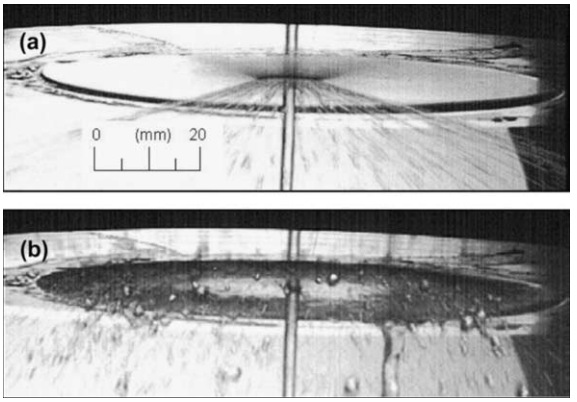

Fig. 3. Sequence of video images during quenching (mat: copper, $T_b = 400$ °C, $\Delta T_{sub} = 20$ K, $u = 3$ m/s). (a) t (=554 s) < t^* (=555 s) and (b) t (=576 s) > t^* (=555 s).

Fig. 3(a) shows just one of the flow patterns observed before movement of the wetting front. As has been reported elsewhere [15], depending on the conditions, the observed flow phenomena can pass through a sequence of stages. If the initial temperature was higher than about 300 °C for a copper block, when the jet first struck the surface an explosive flow pattern where the jet broke into thousands of tiny droplets was observed. As the solid cooled, the flow field became less chaotic and in some cases, liquid droplets could be seen departing in rings from the surface with a frequency of approximately 1000 rings per second. Following this, the angle between the departing droplets and the surface increased and a small conical sheet of liquid appeared. For some conditions, the sheet was clearly visible, but in other cases such as is shown in Fig. 3(a), the sheet broke into droplets very close to the surface.

Accompanying the changes in flow pattern, there were a number of changes in the boiling sound before and after the wetting front movement. Fig. 4 illustrates the recorded sound for a set of conditions where the changes in phenomena were particularly clear. The resident time in this case was about 200 s. During the first 120 s, the explosive flow pattern mentioned above could be observed and the boiling sound was quite loud. Fol-

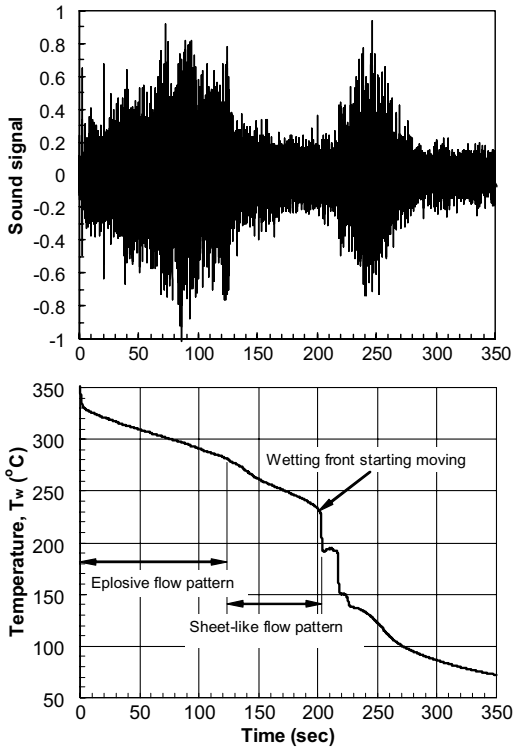

Fig. 4. Sound intensity at 30 cm from the test surface during wetting front propagation [T_w: $r = 5$ mm, copper, $T_b = 350$ °C, $\Delta T_{sub} = 50$ K, $u = 3$ m/s].

lowing this, the sharp splattering sound died down and the experiment became very quiet as the flow pattern changed to the conical liquid sheet. The sheet then disappeared and the wetting front started to move forward. A short time after movement commenced the sound level increased and the sharp boiling sound could be heard again. The loudest sound approximately corresponded to the time of the maximum heat flux for the experiment. Finally the sound diminished as boiling ceased and the mode of heat transfer changed to single-phase convection.

The history of the boiling sound shown in Fig. 4 and the video images have some important implications for the nature of the phase change phenomena before and after the resident time. The sharp splattering sound is most likely the result of some form of nucleate boiling. Now to obtain the liquid superheat and nucleation sites required for nucleate boiling liquid/solid contact is necessary. Thus Fig. 4 indicates that liquid/solid contact occurs long before the movement of the wetting front in what may be described as a kind of transition boiling phenomena [15]. During the first 120 s in Fig. 4, cycles of brief liquid/solid contact followed by separation probably occur at a very high frequency. During the next 80 s, the surface temperature is lower, the phase change is less explosive and solid/liquid contact continues. Visual observations suggested that surface wetting might have been almost continuous in the central region during this time from about 120 s to 200 s but for some reason the wetting front did not move forward.

Towards establishing criteria for defining the time when the wetting front moves forward, in relation to the above observations we can conclude that the resident time does not correspond to the time when the liquid first directly contacts the solid. Nor does it appear to correspond to the time when continuous wetting is first established beneath the jet. Rather the completion of the resident time, t^*, ultimately must relate to overcoming a thermal, hydrodynamic, heat flux or some other balance at the wetting front itself.

Another interesting observation is that in spite of the different flow phenomena during the resident time, the size of the region of interaction between the liquid jet and solid was noted to remain relatively fixed before movement of the wetting front. For the copper block, the radius of this region, r^*, was found to be 5 ± 1 mm for a range of conditions and for brass, $r^* = 8 \pm 3$ mm. For example, in the case shown in Fig. 3, from the time just after the jet struck the surface until 1 s before the wetting front moved as shown in Fig. 3(a), the apparent wetting front remained at a constant radial position ($r^* = 5$ mm).

Finally, the video images show that the resident time can be much larger than the time for the wetting front to move across the surface. For the case in Fig. 3 the resident time was 555 s in contrast to the 22 s required for the wetting front to reach the circumference of the cylinder. A similar trend has been observed for all experimental conditions with a moderately higher value for the resident time and for those cases the resident time was higher than the propagation period by a few times to 100 times.

3.3. Surface temperature and heat flux before and after resident time

Typical surface temperature and heat flux distributions with position and time estimated by Eqs. (2) and (3) respectively are shown in Fig. 5. It is clear from Fig. 5 that the cooling curve can be roughly divided into four regions. These are an initial transient (0–5 s), steady cooling (5–86 s), wetting front movement across the surface (86–106 s) and finally, single-phase convection.

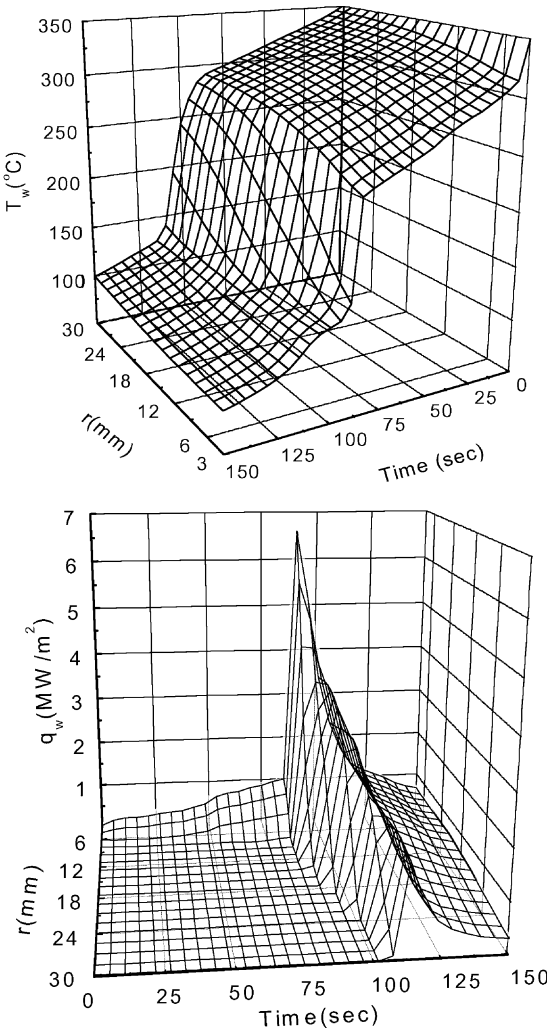

Fig. 5. Estimated surface temperature and heat flux from measured temperatures.

During the first few seconds of the case in Fig. 5 the temperature near the center quickly fell by about 40 °C. This is most likely a transient effect due to the step change in heat flux that occurs when the jet first strikes the center of the test surface. From about 5 s up to the estimated resident time (86 s) the surface temperature dropped at a slow and almost uniform rate with time. Then as the wetting front started moving several major changes took place. The heat flux suddenly increased, the surface temperatures began to fall rapidly and radial temperature gradient became much steeper. During the 20 s that it took for the wetting front to reach the circumference, the entire surface temperature distribution dropped by around 100 °C. Finally both the heat flux and cooling rate diminished as single-phase convection became dominant.

In examining the cooling curves and heat flux distributions there are two key points that we hope to elucidate. The first is what conditions are established at the instant the wetting front starts movement. The second is what factors may influence how long it takes for these conditions to be established. If these two issues can be resolved, much progress can be made towards developing a theoretical model for predicting the resident time.

For the case shown in Fig. 5 it is clear that before movement of the wetting front the temperature near the center is steadily decreasing and the heat flux is steadily increasing. At the instant when the wetting front started moving forward the temperature at the edge of the wetted region ($r = 5$ mm) was 242 °C and the heat flux at this position was about 1 MW/m^2. Rather than constants for every experiment, both of these values are found to be strong functions of the experimental conditions as will be discussed in Section 3.6 below.

A further interesting result that has emerged from consideration of the cooling curves is that the maximum heat flux point always occurred just after movement of the wetting front. In Fig. 5, within 2 or 3 s from when the wetting front started moving, the heat flux increased by a factor of about seven to reach its peak value and the temperature just upstream of the wetting front fell to about 140 °C. For all the experimental conditions, the heat flux increased by a factor in the range from 5 to 60. The temperature at the maximum heat flux point was found to always lie in the range from about 120 °C to 220 °C for all 192 combinations of conditions given in Table 1. However, since the maximum heat flux always occurred after wetting front movement, it may be considered an effect of wetting rather than the direct cause of wetting front movement.

While it appears that a simple set of criteria for wetting front movement is not immediately obvious from the results of different experimental conditions it is worth noting that higher initial solid temperatures almost always resulted in longer resident times. This is strong evidence that factors affecting the overall rate of cooling of the solid at higher temperatures have an important influence on the resident time. During the first 86 s in Fig. 5 the almost steady cooling rate observed will be a function of heat flux to the jet in the central region, the size of the wetted region and losses to the environment surrounding the dry region by single phase convection and radiation. We may expect that the total heat capacity of the block also will be important since for a given total heat flux, the bulk temperature of a larger block will drop more slowly.

3.4. Regimes for wetting delay

An examination of the cooling curves for all of the data indicated that each set of conditions in Table 1 could be classified into one of three regimes for the resident time. We have elected to describe the categories as (a) quick cooling, (b) moderate cooling and (c) slow cooling. Fig. 6 gives typical examples of the three cate-

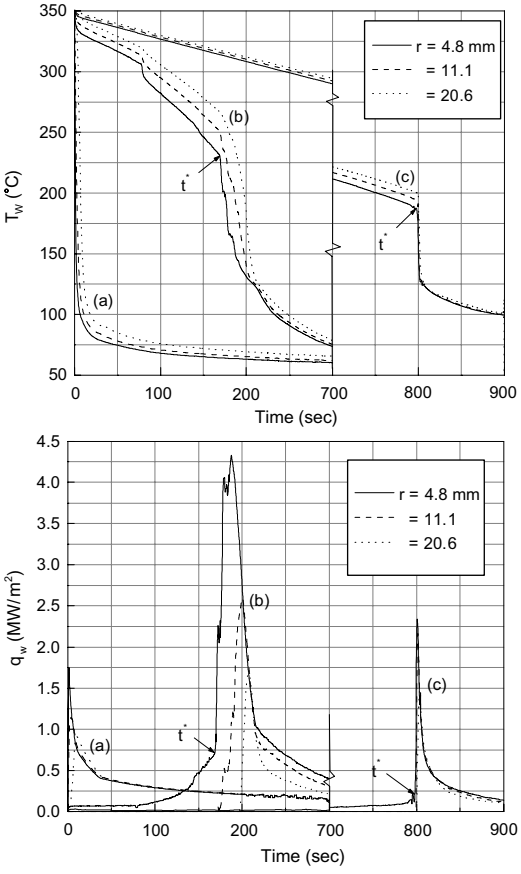

Fig. 6. Cooling curve and heat flux at a position during quenching for copper and carbon steel. (a) Carbon steel: $T_b = 350$ °C, $\Delta T_{sub} = 50$ K, $u = 3$ m/s, (b) Copper: $T_b = 350$ °C, $\Delta T_{sub} = 50$ K, $u = 3$ m/s and (c) Copper: $T_b = 350$ °C, $\Delta T_{sub} = 5$ K, $u = 3$ m/s.

gories. The case (a) in Fig. 6 shows a cooling curve for carbon steel. In this case it took only a fraction of a second for the wetting front to start movement and the surface temperature cooled very rapidly immediately after the jet struck the surface. The case (b) in Fig. 6 shows a moderate cooling case that occurred for a copper block with a jet subcooling of 50 K. In this case the resident time is 170 s and the curves have a slight irregularity at around 80 s, which corresponds to a change in sound and flow pattern described in Section 3.2 (cf. Fig. 4). A slow cooling case (c) is also shown in Fig. 6 where the material is copper and the jet subcooling is 5 K. Here the resident time was 800 s and the cooling rate was almost constant during this time.

In this study, all the measured resident times for steel were a fraction of a second while a large proportion of the results for copper could be classified as either moderate or slow cooling. For the quick cooling situation, the surface temperature drops from its initial temperature to close to the corresponding liquid temperature very soon after jet impingement. During this time, the wetting front begins to move slowly across the surface and the heat flux reaches its maximum value. The different behavior among the three materials is most likely the result of the ability of the material to supply heat to the region of the surface where the liquid contacts the surface. In the case of copper the thermal conductivity is high so that heat can be supplied easily to balance the heat flux demanded by the jet and maintain a high surface temperature. In contrast, the conductivity of carbon steel is about one-tenth that of copper so the surface cools quickly if the heat flux is high.

Another important feature that was different among the three regimes was the spatial temperature gradient at the resident time and during propagation of the wetting front. For shorter resident time regime (a), the radial temperature gradient is quite large at and after the resident time. In contrast, for regime (c) the solid surface temperature is much more uniform. A comparison of the cooling curves at t^* for different radial positions in Fig. 6 shows this. In the case (c) at t^* the difference in temperature between the radial position $r = 4.8$ mm and $r = 20.6$ mm is only about 20 °C. For the case (a) the temperature difference between these two points during movement of the wetting front, for example at about 10 s, is over 100 °C. Therefore, for larger resident times, the temperature gradient in the radial direction is small and the radial propagation of the wetting front (wetting front velocity) is faster. Inversely, we observe that a higher temperature gradient in the radial direction corresponds to slower wetting front velocity for quick cooling conditions.

Finally it is worth mentioning that the period of time between when the wetting front started moving until the maximum heat flux condition was generally greater in the moderate cooling regime (b) than the slow cooling regimes. The curve for the heat flux in the case (b) shows the heat flux peak occurred 18 s after the wetting front started moving where for case (c) this delay was about 5 s.

3.5. Effect of $u\Delta T_{sub}$

A further distinction between the fast and slower cooling regimes and some interesting trends for the resident time becomes clear if the resident time is plotted against the parameter, $u\Delta T_{\mathrm{sub}}$. Fig. 7 shows three different trends that consistently appear for each of the four initial temperatures considered for a copper block. In the case of longer resident times, t^* is a strong function of $u\Delta T_{\mathrm{sub}}$ as shown by the solid lines in Fig. 7. For a resident time between 1 and 30 s (tentatively defined) the trend becomes almost vertical as shown by the dashed lines. This indicates an abrupt change in the resident time within the vicinity of some critical value of $u\Delta T_{\mathrm{sub}}$. For very small resident times less than 1 s the trend changes again as is shown by the dotted lines.

For the different initial temperatures shown in Fig. 7, the general trend is that for higher initial temperatures the curve shifts to the right. Also all curves show a decrease in t^* with an increase in the velocity-subcooling factor. This shows that the resident time increases with an increase in initial temperature. A possible explanation for these features is as follows. Note that both u

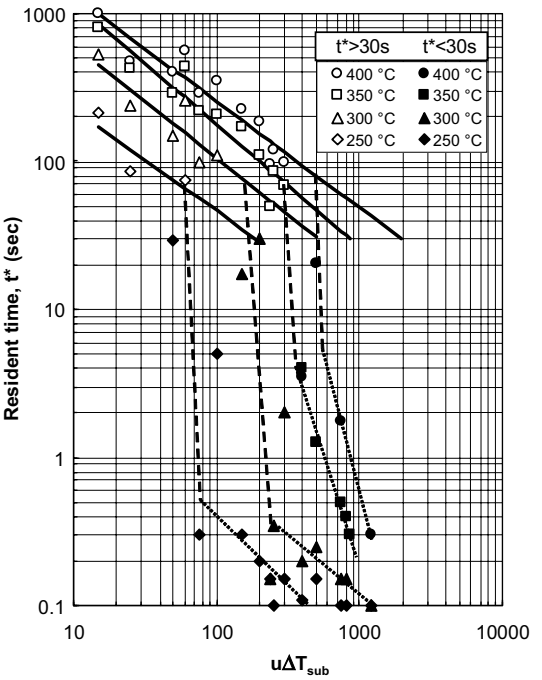

Fig. 7. Variation of resident time for copper with different initial temperature as a function $u\Delta T_{\mathrm{sub}}$.

and ΔT_{sub} are parameters from the liquid side only and that for a given geometry and material, the initial temperature of the solid is an indicator of the quantity of heat initially stored in the solid. Also it is generally found in jet boiling experiments that increasing the jet velocity or increasing the subcooling both lead to higher heat fluxes. Thus the parameter, $u\Delta T_{sub}$, is perhaps one indicator of the ability of the liquid side to extract heat. In other words, a higher value of $u\Delta T_{sub}$ implies a higher heat flux, which makes the solid cool faster leading to shorter resident times. A higher initial temperature roughly means that more heat must be removed before the conditions where the wetting front moves forward are reached. It should be noted however, that this hypothesis does not account for the effect of $u\Delta T_{sub}$ on the temperature at which the wetting front moves forward. This will be discussed in Section 3.6 below.

Another interesting feature in Fig. 7 is that the critical value of $u\Delta T_{sub}$ also increases with an increase in initial temperature. This critical value forms the boundary between the moderate and fast cooling regimes described in Section 3.4. The reason for the sudden change between the regimes is presently unclear. However, it may be that the fast cooling regime is the result of quickly reaching the conditions for wetting front movement during the initial localized transient cooling just after the jet contacts with the surface. This initial transient cooling can be seen in Fig. 5 during the first 5 s near the center of the surface. If, as in Fig. 5, the conditions favorable for wetting front propagation are not reached during this initial period of rapid cooling then the whole solid must cool down before wetting front movement. This results in a much longer resident time.

The results shown in Fig. 7 are for copper only. Similar trends were observed for brass also except that curves were generally to the left of those for copper. For steel, the resident time was less than 1 s for the entire experimental range of the present study. It is suspected however, that should the initial temperature be raised further, the same trends as shown in Fig. 7 will appear for steel also.

3.6. Correlations for surface temperature at wetting front at resident time

Of great importance to the present study are the precise conditions that occur when the wetting front begins to move. From an understanding of the classical boiling curve one would suspect that among all the conditions, the surface superheat at the wetting front is likely to be a key factor. Fig. 8 shows the surface temperature at the resident time at the wetting front ($r = 5$ mm) for the whole range of experimental conditions for copper. Far from being a single constant value however, the temperature, T_w^*, ranges from 170 °C to 385 °C. There is a clear trend in relation to the parameter $u\Delta T_{sub}$ and to the initial temperature of the solid.

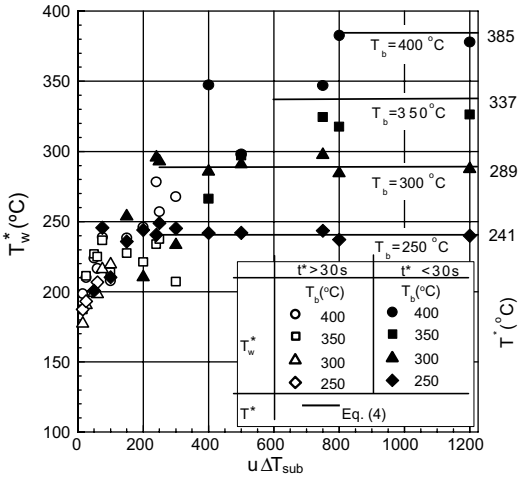

Fig. 8. Variation of surface temperature (at resident time at wetting front) and interface temperature for copper with different initial temperatures.

In Fig. 8, dark symbols are used for data with $t^* < 30$ s. For these shorter resident times the temperature of the wetting front at t^* is almost independent of $u\Delta T_{sub}$ and is a strong function of the initial temperature of the solid. In fact for large values of $u\Delta T_{sub}$ all curves appear to asymptote to values of T_w^* a little below the initial temperature. It is interesting to compare this data with the interface temperature, T^*, estimated from the sudden contact to two semi-infinite bodies. Eq. (4) gives the analytical solution for T^* [19]:

$$T^* = \frac{T_b - T_{liq}}{1 + \sqrt{(\rho c\lambda)_l/(\rho c\lambda)_s}} + T_{liq} \tag{4}$$

Making use of Eq. (4), solid lines are drawn in Fig. 8 for the interface temperature based on the four different initial temperatures. The variation of T^* in Eq. (4) with the variation of T_{liq} from 20 to 95 °C is within 1.5% only due to very small value of $\sqrt{(\rho c\lambda)_l/(\rho c\lambda)_s}$ for copper or brass. Therefore, to avoid almost overlapping of T^* for four values of T_{liq}, T^* for only one T_{liq} (20 °C) has been shown in Fig. 8. The measured temperatures for large values of $u\Delta T_{sub}$ agree quite well with T^*. Thus Eq. (4) may be appropriate for estimating the wetting front temperature at the resident time in cases where the resident time is very short.

The unshaded symbols in Fig. 8 represent experimental data for $t^* > 30$ s. These data are classified as from the moderate or slow cooling regimes in Section 3.4. In the case shown for copper here, this set of data appears to be a strong function of $u\Delta T_{sub}$ but only a weak

function of the initial solid temperature. Thus we can observe from Fig. 8 that the surface temperature at which the wetting front can move forward becomes higher as $u\Delta T_{sub}$ becomes larger until the temperature is close to the interface temperature for the liquid and the solid. At this point the wetting front can move forward almost immediately and the resident time becomes very short. Therefore the parameter $u\Delta T_{sub}$ can be considered to contribute in two ways to shortening the resident time. First, as mentioned in Section 3.5, by increasing the cooling rate of the solid and secondly, by increasing the temperature at which the wetting front can move forward.

The data for copper with $t^* > 30$ s shown in Fig. 8 could perhaps be approximated as a linear function of $u\Delta T_{sub}$. However, a much better correlation which is also applicable for brass with $t^* > 30$ s can be achieved by making T_w^* a function of the initial temperature of the solid, $u\Delta T_{sub}$, and properties of the liquid and solid material. Since from Eq. (4) we suspect the interface temperature may play an important role we have included the dimensionless ratio of $\rho c\lambda$ for liquid and solid. Using the method of least mean squares to determine the constant and the exponents, Eq. (5) gives an empirical correlation for T_w^*.

$$\frac{T_w^* - T_{sat}}{T_b - T_{liq}} = 157\left\{\frac{(\rho c\lambda)_l}{(\rho c\lambda)_s}\right\}^{0.49}\left(\frac{2r^*}{d}\right)^{-0.49} \times (\rho cu\Delta T_{sub})_l^{0.14}(T_b - T_{liq})^{-0.68} \quad (5)$$

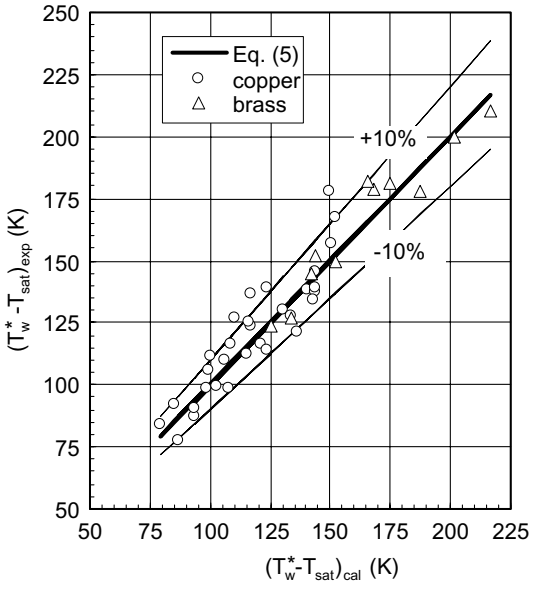

Fig. 9. Experimental data and proposed correlation (for t^*; > 30 s) of surface temperature, T_w^* at resident time at wetting front.

Fig. 9 illustrates how well Eq. (5) represents the experimental data for both copper and brass with resident times greater than 30 s. Most of the data is within ±10% of the proposed relation. Eq. (5) is not non-dimensional because the role of the parameters related to temperature differences is left unclear yet. The meanings of these parameters should be clarified in future studies.

3.7. Correlation for resident time

From the preceding sections, the parameters related to the resident time seem to be $\rho cu\Delta T_{sub}$, $(T_w^* - T_{sat})$, $(T_b - T_{liq})$ and r^*/d. It may be worth mentioning that the heat flux transferred through heat conduction from the solid to liquid is generally proportional to $\sqrt{(\rho c\lambda)_s/t}$ with units [W/m^2 K]. Finally the aim is to predict the resident time, t^*, when the wetting front starts moving. Therefore, we tentatively derive a correlation predicting the resident time based on the above parameters.

$$\frac{\sqrt{(\rho c\lambda)_s/t^*}(T_w^* - T_{sat})}{(\rho cu)_l(T_{sat} - T_{liq})} = 14\left(\frac{2r^*}{d}\right)^{0.72}(\rho cu\Delta T_{sub})_l^{-0.41} \times (T_b - T_{liq})^{-0.99} \quad (6)$$

The temperature (T_w^*) at the wetting front at resident time is obtained from Eq. (5) and then using this temperature the resident time can be predicted with fairly good agreement by Eq. (6) as is shown in Fig. 10. Again the constant and exponents in Eq. (6) were determined by the least mean squares method. Eq. (6) is applicable to all data for copper and brass considered in this study that resulted in resident times greater than 30 s. Eq. (6)

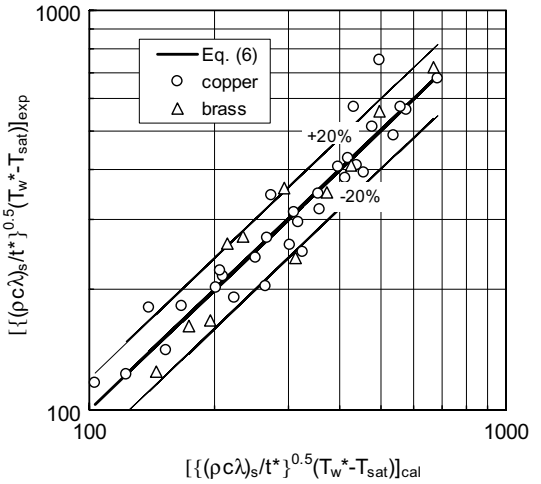

Fig. 10. Experimental data and proposed correlation (for $t^* > 30$ s) of resident time, t^*.

is also dimensional, which should be improved by taking into account parameters related to the temperature differences.

4. Conclusions

With the combination of different means including an inverse solution, visual observation and audible inspection the present study has been conducted to investigate the wetting delay characteristics of jet quenching. Much effort has been given to find out the key parameters responsible for the resident time and temperature at that time. Further comprehensive study is needed for understanding these complicated phenomena. The intrinsic achievements at present from this investigation are summarized as:

1. For moderate/slower cooling condition, the surface temperature drops 100–150 °C within 10–40 s just after the wetting front start moving.
2. The value of maximum heat flux is always attained immediately after the resident time and during the propagation of wetting front movement.
3. The heat flux increases dramatically when the wetting front starts moving. The value of maximum heat flux is 5–60 times higher than the heat transfer value just before the wetting front movement.
4. For moderate/higher resident times, the duration of wetting propagation (the time between when the wetting front starts moving and when it reaches to the end) does not change so much (10–40 s) relative to the resident time for different experimental conditions. The resident time is much larger than the propagation period (it varies from few times to 100 times).
5. Initially (before the wetting front movement) the covered central wetted region has a radius of 5 ± 1 mm for copper and 8 ± 3 mm for brass which was almost constant for whole range of experimental conditions in the present study.
6. Resident time could be categorized in three groups on the basis of a velocity-subcooling factor ($u\Delta T_{sub}$) and the shape of the cooling curves. There also appears to be transition points where the resident time changes suddenly from over 30 s to less than 1 s.
7. The wetting front starts moving when the surface temperature (T^*_w) drops to the corresponding solid–liquid interface temperature (T^*) for very short resident times.
8. The resident time is a strong function of the properties of the solid material and sub-cooling of the jet. It is also a function of the jet velocity and initial surface temperature.
9. The proposed correlations for the resident time and temperature agree well with the corresponding values from the experiment and the inverse solution over certain ranges in the present study.

Acknowledgement

The authors are grateful to associate professor Y. Mitsutake for his valuable suggestions and assistance in conducting the experiment at different stages.

References

[1] R.G. Owen, D.J. Pulling, Wetting delay: film boiling of water jets impinging hot flat metal surfaces, in: T. Nejat Veziroglu (Ed.), Multiphase Transport Fundamentals, Reactor Safety, Applications, vol. 2, Clean Energy Research Institute, University of Miami, 1979, pp. 639–669.
[2] J.D. Bernardin, I. Mudawar, The Leidenfrost point: experimental study and assessment of existing models, ASME J. Heat Transfer 121 (No. 4) (1999) 894–903.
[3] J.D. Bernardin, C.J. Stebbins, I. Mudawar, Mapping of impact and heat transfer regimes of water drops impinging on a polished surface, Int. J. Heat Mass Transfer 40 (2) (1997) 247–267.
[4] D.E. Hall, F.P. Incropera, R. Viskanta, Jet impingement boiling from a circular free-surface jet during quenching. Part 2. Two-phase jet, ASME J. Heat Transfer 123 (No. 4) (2001) 911–917.
[5] J. Filipovic, F.P. Incropera, R. Viskanta, Quenching phenomena associated with a water wall jet. 1. Transient hydrodynamic and thermal conditions, Exp. Heat Transfer 8 (1995) 97–117.
[6] J. Hammad, Y. Mitsutake, M. Monde, Movement of maximum heat flux and wetting front during quenching of hot cylindrical block, Int. J. Thermal Sci. 43 (2004) 743–752.
[7] M. Monde, Y. Katto, Burnout in a high heat flux boiling system with an impinging jet, Int. J. Heat Mass Transfer 21 (1978) 295–305.
[8] X. Liu, J.H. Lienhard V, J.S. Lombara, Convective heat transfer by impingement of circular liquid jets, ASME J. Heat Transfer 113 (1991) 517–582.
[9] D.E. Hall, F.P. Incropera, R. Viskanta, Jet impingement boiling from a circular free-surface jet during quenching. Part 1. Single-phase jet, ASME J. Heat Transfer 123 (2001) 901–910.
[10] H. Lienhard V, X. Liu, L.A. Gabour, Splattering and heat transfer during impingement of a turbulent liquid jet, ASME J. Heat Transfer 114 (No. 2) (1972) 362–372.
[11] B.D.G. Piggott, E.P. White, R.B. Duffy, Wetting delay due to film and transition boiling on hot surfaces, Nucl. Eng. Des. 36 (1976) 169–181.
[12] S. Kumagai, S. Suzuki, Y. Sano, M. Kawazoe, Transient cooling of a hot metal slab by an impingement jet with boiling heat transfer, ASME/JSME Thermal Eng. Conf. 2 (1995).
[13] J. Hammad, Characteristics of heat transfer and wetting front during quenching high temperature surface by jet impingement, Ph.D. thesis, Graduate School of Science and Engineering, Saga University, Japan, 2004.

[14] P.L. Woodfield, M. Monde, A.K. Mozumder, The possibility of homogeneous nucleation boiling during transient liquid/solid contact in a jet impingement quench cooling system, Thermal Sci. Eng. 12 (4) (2004) 39–40.
[15] P.L. Woodfield, M. Monde, A.K. Mozumder, Observations of high temperature impinging-jet boiling phenomena, Int. J. Heat Mass Transfer 48 (2005) 2032–2041.
[16] J. Hammad, M. Monde, Y. Mitsutake, Characteristics of heat transfer and wetting front during quenching by jet impingement, Thermal Sci. Eng. 12 (1) (2004) 19–26.
[17] M. Monde, H. Arima, W. Liu, Y. Mitsutake, J.A. Hammad, An analytical solution for two-dimensional inverse heat conduction problems using Laplace transform, Int. J. Heat Mass Transfer 46 (2003) 2135–2148.
[18] J. Hammad, M. Monde, Y. Mitsutake, H. Arima, Determination of surface temperature and heat flux using inverse solution for two dimensional heat conduction, Thermal Sci. Eng. 10 (2) (2002) 17–26.
[19] H.S. Carslaw, J.C. Jaeger, Conduction of Heat in Solids, second ed., Oxford University Press, 1959, pp. 87–88.